

High sensitive sol-gel based electrochemical immunosensor for Clenbuterol Determination

Benle Zhan, Yeting Zhang, Xiang Zhao *

College of Physical Education, Chengdu University, Chengdu 610106, China

*E-mail: xiangzhaollz@sina.com

Received: 31 July 2021 / *Accepted:* 9 September 2021 / *Published:* 10 October 2021

Clenbuterol is a class of sympathomimetic agents that are used clinically to treat asthma and bronchospasm. It also has physiological effects similar to those of metabolic steroids to promote the growth of muscle tissue, and is therefore abused in animal husbandry to improve lean muscle mass. It is also used as an agonist that has been banned in sports. In this work, a sensitive electrochemical immunosensor was constructed by modifying ZnO nanoparticles and clenbuterol onto the electrode surface using sol-gel method with clenbuterol being the detection target. Under the optimized experimental conditions, the immunosensor showed a wide linear range and low detection limit. The working linear range was 0.3 to 1000 ng/mL, and the detection limit was 0.12 ng/mL. Meanwhile, this immunosensor is simple, rapid, reproducible and stable. In addition, the above sensor has a good accuracy and immunity to interference in the detection of animal feed samples.

Keywords: Clenbuterol; Immunosensor; Sol-gel; Doping; ZnO

1. INTRODUCTION

Currently, doping abuse is prevalent in various fields of sports, food, medicine and health care. In sports games, many individuals as well as teams choose to improve their performance by doping in order to get better results [1,2], which is a serious violation of sports ethics and the principle of fairness in sports games. Moreover, doping can bring lots of side effects to athletes, seriously endangering their physical and mental health. In terms of food safety, drug abuse in the farming industry is the major cause of the frequent occurrence of food safety accidents in recent years, among which doping abuse has become the most prominent problem of livestock products [3,4].

Veterinary drug residues refer to the accumulation and storage of prodrugs, metabolites and drug impurities in cells, tissues and organs after the consumption of drugs to animals [5–7]. The inclusion of

appropriate amounts of veterinary drugs in feed has the effect of reducing animal morbidity and mortality, improving lean meat, and changing the quality of animal products. β -agonist is one of the veterinary drug residues, a type of phenylethanolamine compound [8–10]. The most common β -agonist veterinary drugs include clenbuterol, salbutamol, and terbutaline. In medicine, β -agonist can relieve asthma symptoms by stimulating airway smooth muscle and mast cell receptors on the surface of the mast cell membranes, which can relax airway smooth muscle, reduce mast cells, and increase airway epithelial cilia oscillation [11,12]. A sudden stop of long-term doping may lead to tachycardia, myocardial infarction and even death [13].

The basic detection procedure for β -agonists should include extraction, purification and highly sensitive detection. As different stimulants are present in different forms in metabolic process [14–19], some sample pre-treatments are required depending on the types of stimulants, which often requires the addition of an enzymatic digestion or solvent dissociation conjugate step to the sample. After the pretreatment, the sample needs to undergo further purification, the main methods of which include liquid-liquid extraction, solid-phase extraction, matrix solid-phase dispersion techniques, supercritical fluid extraction, immunoaffinity chromatography and molecular blotting. After purification, the sample can be detected by various methods, such as high performance liquid chromatography, liquid-mass spectrometry, spectrophotometry, gas chromatography, capillary electrophoresis, immunoassay, and electrochemistry [20–26].

Among the detection technologies, sensor technology is one of the most successful and promising detection means. Biosensor is an emerging technology developed in recent years, and has become one of the hot topics for research in life science due to its economical and practical advantages, compact structure, high efficiency, specificity and sensitivity [27–33]. Biosensors are mainly an inter-discipline that is organically combined by the transducer of biofilm and physical chemistry, which is an advanced biotechnology detection method, as well as the rapid trace and analysis of molecular level. Due to the advantages of small size, high accuracy, low cost and low amount of material to be detected, biosensors have been rapidly developed in a number of fields such as bioengineering and medical treatment [34,35].

A biosensor is mainly composed of two parts: a biosensitive element and a transducer. Its selectivity depends mainly on the selection of the sensitive material, while the sensitivity is related to the type of the transducer and the curing technology of the biomaterial. Therefore, the development of curing technology is one of the key factors to improve the performance of the biosensor, and the application of the sol-gel method in biosensors is the chemical modification of electrode mode, in which the bioactive material is added to the sol-gel system and applied dropwise to the electrode surface [36–38]. Sol-gel is conducive to the maintenance of the detector's activity, but it also has porosity, high thermal stability and chemical inertness and good biocompatibility. Compared with traditional methods, the advantages of sol-gel electrochemical biosensors include not only being simple to operate and fast to detect, but also positive chemical and thermal stability, high sensitivity, and good reproducibility. Among the various types of sol-gel, the porous inorganic silica sol-gel has received extensive attention. ZnO materials have prominent strengths and research value in the field of biosensors because of their good biocompatibility and high isoelectric point [39–41]. The emerging research results in recent years have shown that nanostructured ZnO has promising applications in mechanical sensing, optical sensing, gas sensing, biomolecule detection or DNA sensing [42–45].

The source of raw materials for Chitosan (CS) is abundant and it is simple to prepare. It can also be used as a stable matrix for immobilized enzymes, however, the conductivity is not good. Therefore, the application of ZnO and CS together to form an organic-inorganic nanohybrid membrane immobilization can not only improve the stability of the membrane, but also enhance the conductivity and sensitivity of the sensor. In this study, a sensitive electrochemical immunosensor was constructed by modifying ZnO and clenbuterol onto the electrode surface with the sol-gel method, which has the advantages of simplicity, rapidity, good reproducibility and stability.

2. EXPERIMENTAL

2.1. Reagents and Instruments

Zn(CH₃COO)₂•2H₂O, CH₃OCH₂CH₂OH, CH₃CH₂OH, (CH₃)₂CHOH, H₂NCH₂CH₂OH, HN(CH₂CH₂OH)₂, bovine serum albumin were purchased from Macklin Co. Clenbuterol kit was purchased from Beijing Wanger Biotechnology Co. All other reagents were analytical grade and could be used without further purification. All electrochemical tests were performed at the VersaSTAT 3 electrochemical workstation. A three-electrode system was adopted for testing, including a platinum wire counter electrode, an Ag/AgCl reference electrode and a modified glassy carbon working electrode. Crystal structure analysis of the prepared ZnO films was performed with a two-crystal X-ray diffractometer (X'Pert Pro, Philips). Photoluminescence measurements of ZnO thin films were performed with a Jobin Yvon LABRAM-HR model structural confocal microspectrometer. The surface morphology of ZnO films was observed by field emission scanning electron microscopy, JEOL-JSM-6700F. The DTG-60H thermogravimetric-differential thermal analyser manufactured by SHIMADZU, Japan was adopted for thermogravimetric analysis.

2.2. Construction of sensing interface

The zinc acetate dihydrate was accurately weighed on an electronic balance and placed in a corked triangular flask in approximately 30 mL of ethanol solvent. After 10 min, 4.60 mL of ethanolamine stabilizer was added and stirred for 10 min. After it was cool, ethanol was titrated in a 50 mL volumetric flask to prepare a 0.75 M sol. Finally, the solution was stirred for 1 h at 70°C on a magnetic stirrer to form a homogeneous and transparent solution, which was allowed to stand for at least 48 h before use. Under the same conditions, 0.75 M ZnO precursor sols were prepared using isopropyl alcohol (IPA) and ethylene glycol methyl ether (EGME) as solvents, respectively, and thus ZnO sols were prepared with three different solvents. ZnO sols prepared with ethanol, isopropanol and glycol methyl ether were denoted as ZnOeth, ZnOme and ZnOgme.

The GCE electrode was polished with 1.0, 0.3 and 0.05 μm Al₂O₃ powder, and cleaned with 1:1 nitric acid solution, anhydrous ethanol and secondary distilled water for 3 min each. 2 mg/mL clenbuterol solution at pH 7.00 and ZnO sol-gel were mixed 1:1 by volume. A certain amount of ZnO-clenbuterol mixture was applied dropwise to the surface of GCE, and 2 μL of 1 % chitosan (CS, 2% acetic acid)

solution was applied dropwise to the electrode surface after natural drying (denoted as clenbuterol-ZnO/GCE). ZnO sol-gel modified GCE without being mixed with clenbuterol was denoted as ZnO/CGE. After 12 h, 5% bovine serum albumin (BSA) was used to seal the non-specific active sites on the surface of the modified electrodes, which were then immersed into 200 μL of a mixture of clenbuterol antibody and clenbuterol to be measured (denoted as anti/clenbuterol-ZnO/GCE). Figure 1 shows the schematic diagram of the preparation of immunosensor. Electrochemical sensing was performed in phosphate buffer (PBS) containing 2 mM $\text{K}_3[\text{Fe}(\text{CN})_6]$. The current response of the immunosensor was recorded with the differential pulse voltammetry (DPV).

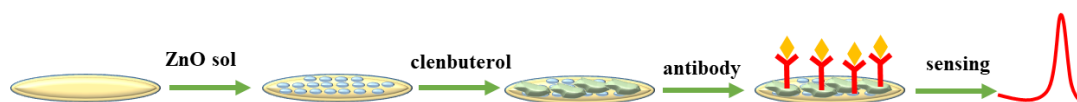


Figure 1. Schematic diagram of immunosensor fabrication.

3. RESULTS AND DISCUSSION

A certain amount of ZnO sols prepared with different solvents were tested in thermal analysis experiments. As shown in Figure 1A, the sols prepared with the three different solvents were more or less the same except for the different positions of heat absorption peaks at the beginning. The boiling points of ethanol, isopropanol and glycol methyl ether are 78.4°C, 82.3°C and 124.5°C, respectively, the reason for which is that their boiling points are the starting temperature of evaporation, and the temperature corresponding to a large amount of evaporation is not the same as their boiling points. In addition, water and other organic substances also evaporate or absorb heat in the meantime, which inevitably affects the position of its maximum heat absorption peak. The boiling point of ethanolamine is 173°C while there are small thermal changes around 230°C and 270°C, which can be considered as corresponding to the absorption as well as the melting and decomposition of zinc acetate monomer. It is in agreement with the previously reported results [46]. The most obvious change in the spectrum is a clear exothermic peak near 375 °C, while no mass change exists in the thermogravimetric analysis. The exotherm is considered to be the point of crystallization of the ZnO film, i.e., the transition from the disordered to the ordered state. Since ethanolamine is basic, zinc acetate is easy to be partially hydrolyzed first under these conditions and produces $\text{Zn}(\text{OH})_2$, which generates ZnO particles in the case of thermal decomposition. The reaction kinetics and principles regarding the ZnO precursors are treated for further analysis.

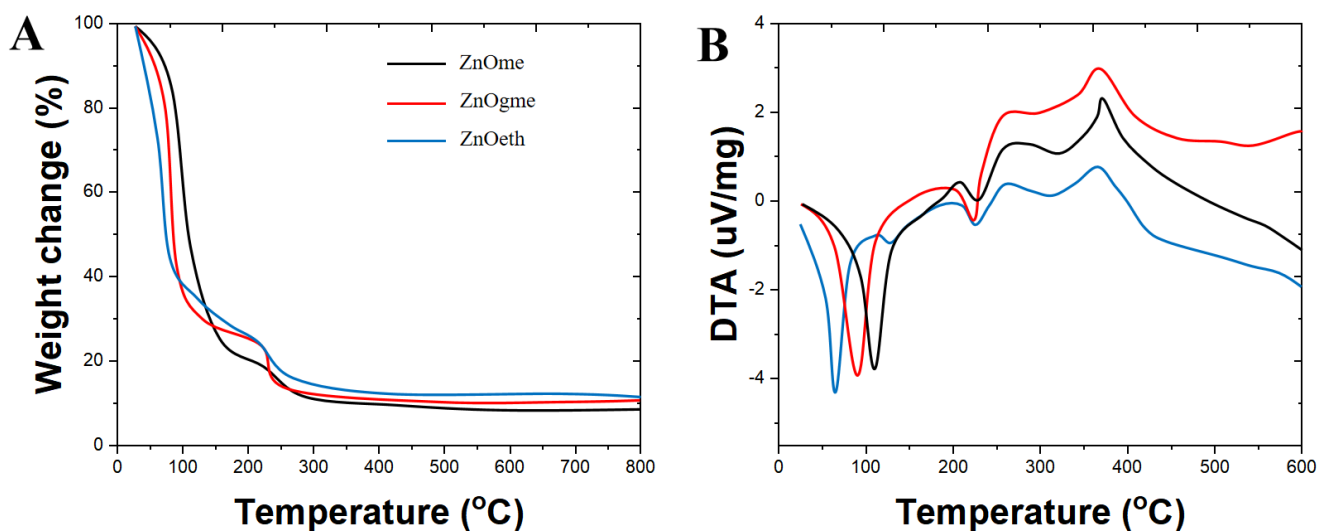


Figure 2. (A) Thermogravimetric analysis and (B) thermal difference analysis of ZnOeth, ZnOme and ZnOgme.

Figure 3 shows the XRD patterns of ZnOeth, ZnOme and ZnOgme, from which it can be obviously noted that the highest peak is located near 34.5° corresponding to the (002) planes of the all ZnO films, which are different from the strongest peak (101) plane of the ZnO powder diffraction peak, indicating that a ZnO film is produced instead of powder. The rest of the peaks correspond to the (001), (101), (102) and (110) diffraction planes of the all ZnO films in that order. ZnO exists in three crystal lattice structures, i.e. wurtzite, zinc blende, and rock salt [47]. The lattice planes found in our spectra correspond to the hexagonal wurtzite structure of ZnO. It can also be seen from the figure that all the samples have a certain selective orientation, and the selective growth of ZnO is related to the magnitude of the surface energy of each face, which is calculated to be the lowest on the (002) face of ZnO, while all the other faces have higher surface energy than this face, thus the ZnO films generally grow selectively along the (002) face.

To further investigate the surface morphology and grain size of ZnO films prepared with different solvents as solutes, ZnOeth, ZnOme and ZnOgme were characterized by SEM. As shown in Figure 4, it is clear that at this magnification the ZnOeth, ZnOme have many large grooves, while the ZnOgme surfaces tested under the same conditions are relatively homogeneous. The formation of ZnO structures with respect to the solvent type can be explained by understanding the solvent-driven shape-controlled crystal growth process [48]. The polarity and chemical nature of the organic solvent in each reaction mixture may act as a selective adhesion surfactant to facilitate the process of shape-controlled crystal growth [49].

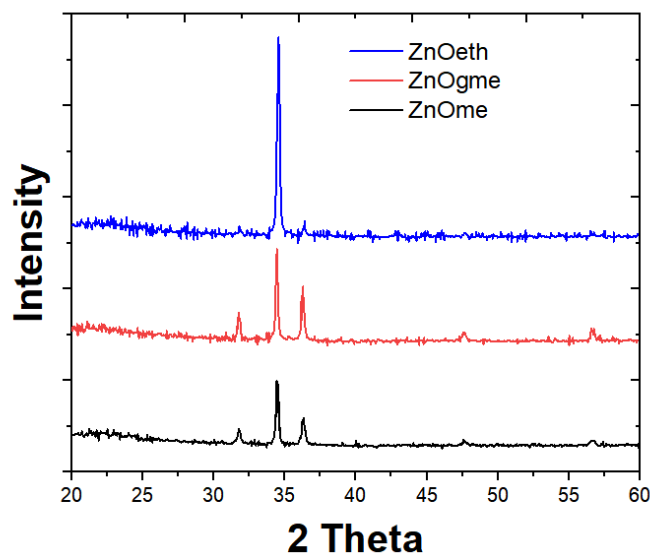


Figure 3. XRD patterns of ZnOeth, ZnOme and ZnOgme.

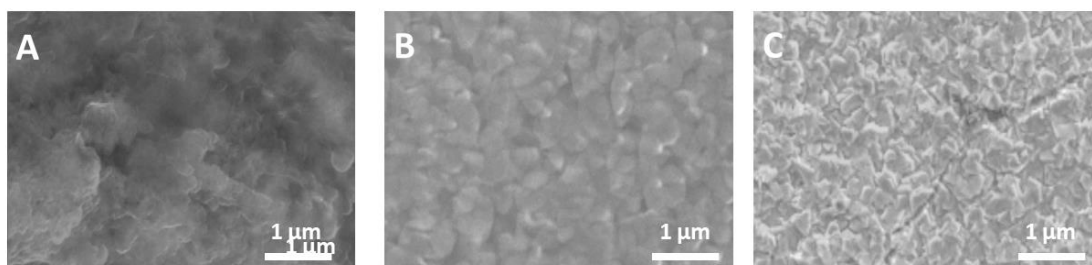


Figure 4. SEM images of (A) ZnOeth, (B) ZnOme and (C) ZnOgme.

In general, the optimized temperature for immune reactions is 37°C, which was therefore utilized as the optimal temperature in this study. In addition, in order to have the maximum current response of the sensor in detecting the samples, we investigated the effect of ZnOeth, ZnOme and ZnOgme on the current at different antibody concentrations and antibody incubation times. Electrochemical sensing was performed in PBS containing 2 mM $K_3[Fe(CN)_6]$, and the current response of the immunosensor was recorded with the DPV. As shown in Figure 5, the current response of the three sensors decreases with the increase of antibody incubation time. The current of all sensors reached a steady state after almost 40 min. Comparing the three sensors, it can be noted that the sensor with ZnOme as the solvent had the largest change in current. Therefore, the ZnOme was used for the follow-up study.

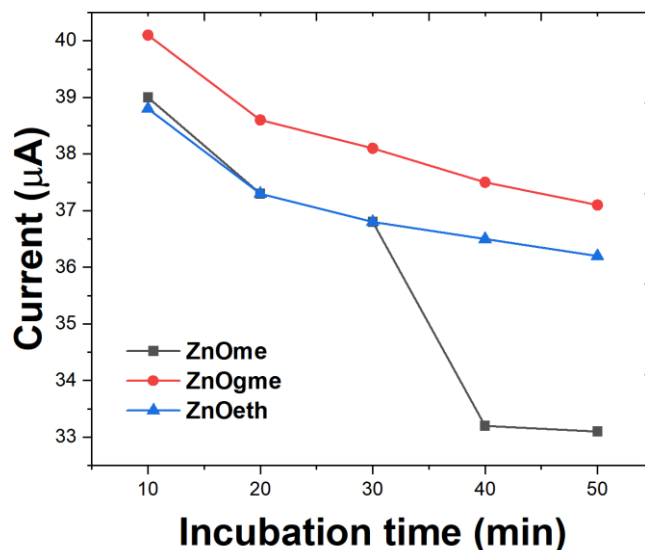


Figure 5. Effect of incubation time of three immunosensors in pH 7.2 PBS solution containing 2 mM $K_3[Fe(CN)_6]$.

Cyclic voltammetry was adopted to study the changes in electrochemical behavior of the electrode surface using $K_3[Fe(CN)_6]$ as a probe. Figure 6 shows the cyclic voltammograms of the antibody, clenbuterol and ZnO modified electrode in 2 mM $K_3[Fe(CN)_6]$. The current response of the ZnO-modified GCE has a significant increase compared to bare GCE, and the peak current gradually decreased when clenbuterol, HRP and antibodies were solidly loaded. The reason for the phenomenon of current drop is that the clenbuterol and antigen-antibody complexes are insulating, which hinders the diffusion of the redox probe to the electrode surface [50].

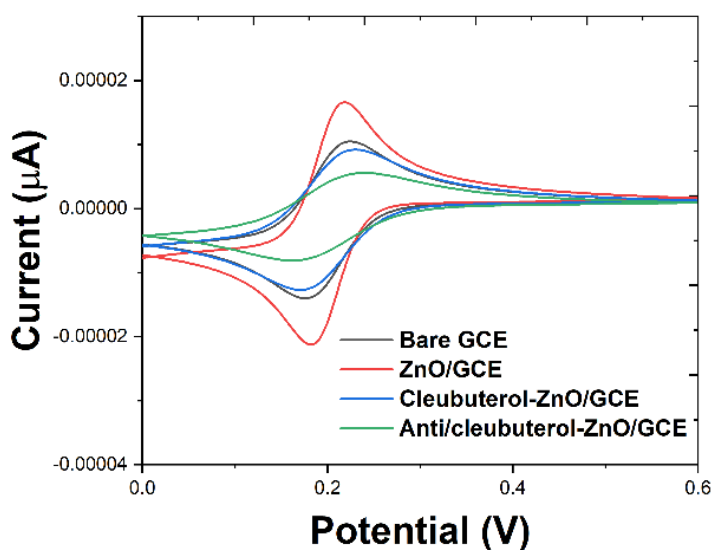


Figure 6. CV of bare GCE, ZnO/GCE, clenbuterol-ZnO/GCE, anti/cleubuterol-ZnO/GCE in pH 7.2 PBS solution containing 2 mM $K_3[Fe(CN)_6]$. Scan rate: 50 mV/s.

The performance of the constructed immunosensor was evaluated under optimized conditions with the DPV assay for clenbuterol standards (0.3 ng/mL, 0.9 ng/mL, 2.7 ng/mL, 8.1 ng/mL, 1000 ng/mL and 1000 ng/mL). Based on the principle of competitive immunoassay, a conclusion can be drawn that the DPV response current of the immunosensor decreases as the concentration of clenbuterol in the culture medium increases. Therefore, the higher the concentration of clenbuterol to be measured is, the less the antibody complexes are bound to the electrode. The experimentally obtained operating curve is shown in Figure 7, where the logarithmic value of clenbuterol concentration is inversely proportional to its response current for concentration in the range of 0.3-1000 ng/mL and is fitted with the regression equation $I_p(\mu A) = 10.43629c(\mu M) + 30.42638$ with a correlation coefficient ($R^2=0.9841$). The detection limit is calculated as 0.12 ng/mL. Table 1 shows the comparison of detection limit and linear range values of the anti/clenbuterol-ZnO/GCE with other clenbuterol sensors.

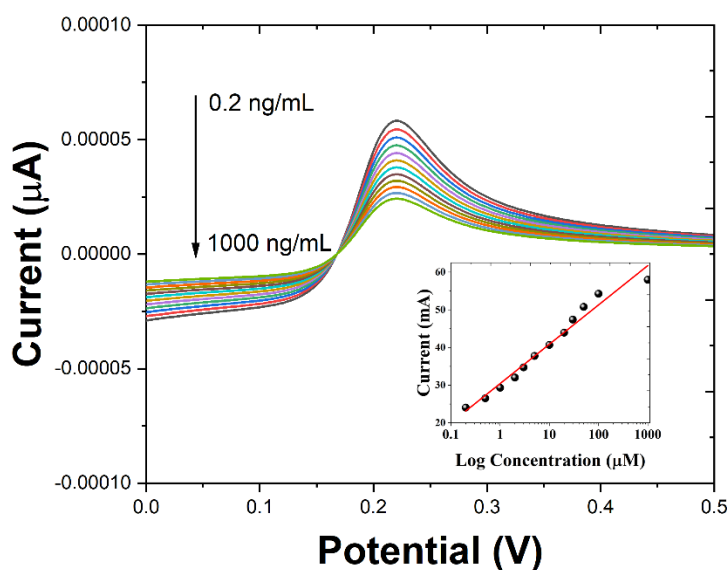


Figure 7. DPVs of the immunosensor after incubated in PBS buffer containing antibody and 0.2 ng/mL, 0.5 ng/mL, 1 ng/mL, 2 ng/mL, 3 ng/mL, 5 ng/mL, 10 ng/mL, 20 ng/mL, 30 ng/mL, 50 ng/mL, 100 ng/mL, 1000 ng/mL clenbuterol. Amplitude: 50 mV; Pulse width: 0.05 s; Pulse period: 0.5 s. Inset: Calibration curves of $\log_{concentration}$ vs. current.

Table 1. Comparison performance of anti/clenbuterol-ZnO/GCE with other clenbuterol electrochemical sensors.

Sensor	LDR	LOD	Ref.
Kudzu vine biochar	0.5-20 ng/mL	0.20 ng/mL	[51]
DNA/RGO-Nafion	2-2000 ng/mL	0.75 ng/mL	[52]
MoS ₂ -Au-PEIhemin	5-50 ng/mL	2 ng/mL	[53]
IP-Nf (BP)	7-780 ng/mL	3.44 ng/mL	[54]
ZnSQD@PANI	1-1000 ng/mL	0.51 ng/mL	[55]
anti/cleubuterol-ZnO/GCE	0.3-1000 ng/mL	0.12 ng/mL	This work

Selectivity is one of the performance indicators of a biosensor that utilizes biomolecules as recognition elements. The effect of interferences on the constructed sensor was explored in this study. When the incubation solution contained 100 ng/mL of ractopamine, the peak current obtained was not significantly different from the current response with the only presence of antibody, indicating that the obtained immunosensor has a good selectivity in detecting clenbuterol.

To further investigate the feasibility of the immunosensor, this sensor was adopted in the detection of clenbuterol in pig feed. The samples were spiked with different concentrations of clenbuterol standard solution and assayed. The results are shown in Table 2, and the recoveries of the spiked samples range from 89.3% to 92.5%, which indicates that the constructed immunosensor has a high accuracy and can be applied to the actual sample detection.

Table 2. Recoveries of clenbuterol from the spiked feed samples.

Add (ng/mL)	Detected (ng/mL)	Recovery (%)
1.00	0.99	99.00
2.00	1.96	98.00
5.00	5.03	100.60
10.00	10.12	101.20

4. CONCLUSION

In this study, ZnO and clenbuterol were modified to the electrode surface with sol-gel method, after which the immunosensor was constructed to detect clenbuterol with the specific binding of antigen and antibody. The optimized conditions allowed the sensor to detect the logarithmic value of clenbuterol concentration linearly in the range of 0.3-1000 ng/mL. The limits of detection were calculated to be 0.12 ng/mL. In conclusion, the constructed immunosensor has a good accuracy, high sensitivity, acceptable stability and good reusability.

ACKNOWLEDGEMENTS

This work was supported by Sichuan Science and Technology Program (2020YFH0184).

References

1. X. Jiang, W. Pan, M. Chen, Y. Yuan, L. Zhao, *Dalton Trans.*, 49 (2020) 6097.
2. R. Lv, E. Wu, R. Wu, W. Shen, C. Ma, R. Shi, R. Guo, M. Shao, J. Liu, *J. Mater. Chem. B*, 8 (2020) 7792.
3. L. Ma, A. Nilghaz, J.R. Choi, X. Liu, X. Lu, *Food Chem.*, 246 (2018) 437.
4. B. Velasco-Bejarano, J. Bautista, M.E. Rodríguez, R. López-Arellano, R. Arreguín-Espinosa, R.V.

- Carrillo, *J. Anal. Toxicol.*, 44 (2020) 237.
5. Z. Wang, J. Jing, Y. Ren, Y. Guo, N. Tao, Q. Zhou, H. Zhang, Y. Ma, Y. Wang, *Mater. Lett.*, 234 (2019) 212.
 6. A. Benedetto, M. Pezzolato, E. Robotti, E. Biasibetti, A. Poirier, G. Dervilly, B. Le Bizec, E. Marengo, E. Bozzetta, *Food Control*, 128 (2021) 108149.
 7. L. Wang, H. Zhang, L. Su, X. Yao, Z. Wang, M. Zhao, J. Sun, J. Wang, D. Zhang, *Sens. Actuators B Chem.*, 331 (2021) 129443.
 8. Y. Sun, H. Chen, P. Ma, J. Li, Z. Zhang, H. Shi, X. Zhang, *Anal. Bioanal. Chem.*, 412 (2020) 193.
 9. C. Zhu, G. Zhao, W. Dou, *Sens. Actuators B Chem.*, 266 (2018) 392.
 10. D.C. Kabiraz, K. Morita, K. Sakamoto, M. Takahashi, T. Kawaguchi, *Talanta*, 186 (2018) 521.
 11. T. Peng, J. Wang, S. Zhao, Y. Zeng, P. Zheng, D. Liang, G.M. Mari, H. Jiang, *Anal. Chim. Acta*, 1040 (2018) 143.
 12. N. Duan, S. Qi, Y. Guo, W. Xu, S. Wu, Z. Wang, *LWT*, 134 (2020) 110017.
 13. S. Piña-Olmos, M. Dolores-Hernández, A. Villaseñor, R. Díaz-Torres, E.R. Bribiesca, R. López-Arellano, P. Ramírez-Noguera, *J. Pharm. Biomed. Anal.*, 195 (2021) 113817.
 14. M. Lv, Y. Liu, J. Geng, X. Kou, Z. Xin, D. Yang, *Biosens. Bioelectron.*, 106 (2018) 122.
 15. Z. Ma, Q. Wang, N. Gao, H. Li, *Microchem. J.*, 157 (2020) 104911.
 16. J. Zhou, Y. Zheng, J. Zhang, H. Karimi-Maleh, Y. Xu, Q. Zhou, L. Fu, W. Wu, *Anal. Lett.*, 53 (2020) 2517.
 17. B. Fan, Q. Wang, W. Wu, Q. Zhou, D. Li, Z. Xu, L. Fu, J. Zhu, H. Karimi-Maleh, C.-T. Lin, *Biosensors*, 11 (2021) 155.
 18. Y. Xu, Y. Lu, P. Zhang, Y. Wang, Y. Zheng, L. Fu, H. Zhang, C.-T. Lin, A. Yu, *Bioelectrochemistry*, 133 (2020) 107455.
 19. L. Fu, Y. Zheng, P. Zhang, H. Zhang, M. Wu, H. Zhang, A. Wang, W. Su, F. Chen, J. Yu, W. Cai, C.-T. Lin, *Bioelectrochemistry*, 129 (2019) 199.
 20. C. Gu, P. Ren, F. Zhang, G. Zhao, J. Shen, B. Zhao, *ACS Omega*, 5 (2020) 5548.
 21. B. Zhang, X. Fan, D. Zhao, *Polymers*, 11 (2019) 17.
 22. W. Long, Y. Xie, H. Shi, J. Ying, J. Yang, Y. Huang, H. Zhang, L. Fu, *Fuller. Nanotub. Carbon Nanostructures*, 26 (2018) 856.
 23. L. Fu, Q. Wang, M. Zhang, Y. Zheng, M. Wu, Z. Lan, J. Pu, H. Zhang, F. Chen, W. Su, *Front. Chem.*, 8 (2020) 92.
 24. L. Fu, K. Xie, Y. Zheng, L. Zhang, W. Su, *Electronics*, 7 (2018) 15.
 25. L. Fu, Y. Zheng, P. Zhang, J. Zhu, H. Zhang, L. Zhang, W. Su, *Electrochem. Commun.*, 92 (2018) 39.
 26. M. Zhang, B. Pan, Y. Wang, X. Du, L. Fu, Y. Zheng, F. Chen, W. Wu, Q. Zhou, S. Ding, *ChemistrySelect*, 5 (2020) 5035.
 27. Q. Huang, T. Bu, W. Zhang, L. Yan, M. Zhang, Q. Yang, L. Huang, B. Yang, N. Hu, Y. Suo, *Food Chem.*, 262 (2018) 48.
 28. Q. Wang, J. Deng, Y. Chen, Y. Luo, X. Jiang, *Chin. Chem. Lett.*, 31 (2020) 1835
 29. X. Hu, H. Zhang, S. Chen, R. Yuan, J. You, *Anal. Bioanal. Chem.*, 410 (2018) 7881.
 30. R. Yang, B. Fan, S. Wang, L. Li, Y. Li, S. Li, Y. Zheng, L. Fu, C.-T. Lin, *Micromachines*, 11 (2020) 967.
 31. L. Fu, K. Xie, D. Wu, A. Wang, H. Zhang, Z. Ji, *Mater. Chem. Phys.*, 242 (2020) 122462.
 32. Y. Zheng, J. Zhu, L. Fu, Q. Liu, *Int J Electrochem Sci*, 15 (2020) 9622.
 33. G. Liu, X. Yang, H. Zhang, L. Fu, *Int J Electrochem Sci*, 15 (2020) 5395.
 34. X. Jin, G. Fang, M. Pan, Y. Yang, X. Bai, S. Wang, *Biosens. Bioelectron.*, 102 (2018) 357.
 35. Y. Cong, H. Dong, X. Wei, L. Zhang, J. Bai, J. Wu, J.X. Huang, Z. Gao, H. Ueda, J. Dong, *Ecotoxicol. Environ. Saf.*, 182 (2019) 109473.
 36. W. Huang, E. Guo, J. Li, A. Deng, *Analyst*, 146 (2021) 296.
 37. H. Malekzad, P.S. Zangabad, H. Mohammadi, M. Sadroddini, Z. Jafari, N. Mahlooji, S. Abbaspour,

- S. Gholami, M.G. Houshangi, R. Pashazadeh, *TrAC Trends Anal. Chem.*, 100 (2018) 116.
38. T. Bu, M. Zhang, X. Sun, Y. Tian, F. Bai, P. Jia, Y. Bai, T. Zhe, L. Wang, *Sens. Actuators B Chem.*, 299 (2019) 126969.
39. N.A.A. Talib, F. Salam, N.A. Yusof, S.A.A. Ahmad, M.Z. Azid, R. Mirad, Y. Sulaiman, *RSC Adv.*, 8 (2018) 15522.
40. K. Zhang, Y. Ge, S. He, F. Ge, Q. Huang, Z. Huang, X. Wang, Y. Wen, B. Wang, *Int J Electrochem Sci*, 15 (2020) 7326.
41. M. Hossain, K. Morita, T. Kawaguchi, *Orient. J. Chem.*, 34 (2018) 1355.
42. J. Neng, Q. Zhang, P. Sun, *Biosens. Bioelectron.* (2020) 112480.
43. X. Yao, Z. Wang, L. Dou, B. Zhao, Y. He, J. Wang, J. Sun, T. Li, D. Zhang, *Sens. Actuators B Chem.*, 289 (2019) 48.
44. L. Wu, Y. Xianyu, Z. Wang, Y. Dong, X. Hu, Y. Chen, *Anal. Chem.*, 91 (2019) 15555.
45. B. Chen, J. Liu, S. Li, Y. Ren, Y. Yuan, H. Zhu, H. Li, *Electroanalysis*, 32 (2020) 2299.
46. K. Davis, R. Yarbrough, M. Froeschle, J. White, H. Rathnayake, *RSC Adv.*, 9 (2019) 14638.
47. T. Beduk, E. Bihar, S.G. Surya, A.N. Castillo, S. Inal, K.N. Salama, *Sens. Actuators B Chem.*, 306 (2020) 127539.
48. L. Ouarez, A. Chelouche, T. Touam, R. Mahiou, D. Djouadi, A. Potdevin, *J. Lumin.*, 203 (2018) 222.
49. T. Saidani, M. Zaabat, M. Aida, R. Barille, M. Rasheed, Y. Almohamed, *J. Mater. Sci. Mater. Electron.*, 28 (2017) 9252.
50. G. Gasparotto, J.P.C. Costa, P.I. Costa, M.A. Zaghete, T. Mazon, *Mater. Sci. Eng. C*, 76 (2017) 1240–1247.
51. K. Zhang, Y. Ge, S. He, F. Ge, Q. Huang, Z. Huang, X. Wang, Y. Wen, B. Wang, *Int J Electrochem Sci*, 15 (2020) 7326.
52. Z. Lotfi, H.Z. Mousavi, S.M. Sajjadi, *Anal. Methods*, 9 (2017) 4504.
53. Y. Yang, H. Zhang, C. Huang, D. Yang, N. Jia, *Biosens. Bioelectron.*, 89 (2017) 461.
54. Y. Ge, M. Qu, L. Xu, X. Wang, J. Xin, X. Liao, M. Li, M. Li, Y. Wen, *Microchim. Acta*, 186 (2019) 1.
55. Z. Zhang, F. Duan, L. He, D. Peng, F. Yan, M. Wang, W. Zong, C. Jia, *Microchim. Acta*, 183 (2016) 1089.